EBioMedicine 43 (2019) 188–200

Contents lists available at ScienceDirect

EBioMedicine

journal homepage: www.ebiomedicine.com

EBioMedicine
Published by THE LANCET

Overexpression of PIMREG promotes breast cancer aggressiveness *via* constitutive activation of NF-κB signaling

Lili Jiang [a,1], Liangliang Ren [a,b,1], Xiaolan Zhang [a,1], Han Chen [a,1], Xuhong Chen [a], Chun Lin [a], Lan Wang [c], Ning Hou [d], Jinyuan Pan [a], Zhongqiu Zhou [a], Hongbiao Huang [a], Danping Huang [e], Jianan Yang [a,f], Yingying Liang [a,g], Jun Li [a,b,*]

[a] *Affiliated Cancer Hospital & Institute of Guangzhou Medical University, Key Laboratory of Protein Modification and Degradation, State Key Laboratory of Respiratory Disease, School of Basic Medical Sciences, Guangzhou Medical University, Guangzhou 511436, China*
[b] *Department of Biochemistry, Zhongshan School of Medicine, Sun Yat-sen University, Guangzhou 510080, China*
[c] *Department of Pathogen Biology and Immunology, School of Basic Courses, Guangdong Pharmaceutical University, Guangzhou 510006, China*
[d] *Key Laboratory of Molecular Target & Clinical Pharmacology, School of Pharmaceutical Sciences & the Fifth Affiliated Hospital, Guangzhou Medical University, Guangzhou 511436, China*
[e] *Department of Ultrasonography, Guangzhou Women and Children's Medical Center, Guangzhou Medical University, Guangzhou 510623, China*
[f] *Department of Urologic Oncosurgery, Affiliated Cancer Hospital & Institute of Guangzhou Medical University, Guangzhou 510095, China*
[g] *Department of Radiation Oncology, Affiliated Cancer Hospital & Institute of Guangzhou Medical University, Guangzhou 510095, China*

ARTICLE INFO

Article history:
Received 3 January 2019
Received in revised form 1 April 2019
Accepted 1 April 2019
Available online 9 April 2019

Keywords:
PIMREG
Breast cancer
NF-κB
IκBα
Negative feedback loop

ABSTRACT

Background: It is well-established that activation of nuclear factor-kappa B (NF-κB) signaling plays important roles in cancer development and progression. However, the underlying mechanism by which the NF-κB pathway is constitutively activated in cancer remains largely unclear. The present study aimed to investigate the effect of PICALM interacting mitotic regulator (PIMREG) on sustaining NF-κB activation in breast cancer.

Methods: The underlying mechanisms in which PIMREG-mediated NF-κB constitutive activation were determined *via* immunoprecipitation, EMSA and luciferase reporter assays. The expression of PIMREG was examined by quantitative PCR and western blotting analyses and immunohistochemical assay. The effect of PIMREG on aggressiveness of breast cancer cell was measured using MTT, soft agar clonogenic assay, wound healing and transwell matrix penetration assays *in vitro* and a Xenografted tumor model *in vivo*.

Findings: PIMREG competitively interacted with the REL homology domain (RHD) of NF-κB with IκBα, and sustained NF-κB activation by promotion of nuclear accumulation and transcriptional activity of NF-κB *via* disrupting the NF-κB/IκBα negative feedback loop. PIMREG overexpression significantly enhanced NF-κB transactivity and promoted the breast cancer aggressiveness. The expression of PIMREG was markedly upregulated in breast cancer and positively correlated with clinical characteristics of patients with breast cancer, including the clinical stage, tumor-node-metastasis classification and poorer survival.

Interpretation: PIMREG promotes breast cancer aggressiveness *via* disrupting the NF-κB/IκBα negative feedback loop, which suggests that PIMREG might be a valuable prognostic factor and potential target for diagnosis and therapy of metastatic breast cancer.

Fund: The science foundation of China, Guangdong Province, Guangzhou Education System, and the Science and Technology Program of Guangzhou.

1. Introduction

Since its discovery about thirty years ago, tremendous progress has been made in understanding the functions and signaling networks of NF-κB in physiological and pathophysiological processes, including inflammation, immunity and cell survival [1]. In line with its central roles in multi-layered physiological functions, deregulated NF-κB activity is found in a large number of diseases, especially in large variety of human malignancies [2–4]. For instance, it has been demonstrated

* Corresponding author at: Affiliated Cancer Hospital & Institute of Guangzhou Medical University, Key Laboratory of Protein Modification and Degradation, State Key Laboratory of Respiratory Disease, School of Basic Medical Sciences, Guangzhou Medical University, Guangzhou 511436, China.
E-mail address: lijun37@mail.sysu.edu.cn (J. Li).
[1] These authors contributed equally to this work.

https://doi.org/10.1016/j.ebiom.2019.04.001

Research in context

Evidence before this study

Nuclear factor-kappa B (NF-κB) has been recognized as one most pleiotropic transcription factor that controls the development of physiological and pathological conditions, such as cancer development and progression. The negative feedback loop formed by NF-κB and its natural inhibitors, IκBs, are believed to play a key role in regulating the NF-κB activity. NF-κB-induced *de novo* resynthesis of intracellular IκB re-shuttles the NF-κB complex from the nucleus to the cytoplasm and thereby prevents hyperactivation of NF-κB. How the NF-κB/IκB negative feedback loop is disrupted in cancer cells, which results in maintaining NF-κB signaling in constitutive activated form, remains largely unknown.

Added value of this study

In the present study, we reported that PIMREG contributed to promote NF-κB activation by sustaining nuclear location and transcriptional activity of NF-κB *via* disrupting the NF-κB/IκBα negative feedback loop. Mechanistically, PIMREG competitively interacted with the Re1 homology domain (RHD) of NF-κB, which is the domain mostly responsible for IκBα interaction. Furthermore, PIMREG was highly expressed in breast cancer and correlated positively with shorter survival of patients with breast cancer. Ectopic expression of PIMREG promoted the breast cancer cell proliferation, migration, and invasive capability. Importantly, silencing of PIMREG significantly reduced the NF-κB transactivity and inhibited the breast cancer aggressiveness.

Implications of all the available evidence

Our study demonstrated that PIMREG promoted breast cancer aggressiveness *via* constitutive activation of NF-κB signaling, and was a valuable prognostic factor and a potential target for the diagnosis and therapy of metastatic breast cancer.

that hyperactivation of NF-κB signaling elicits promotion of migration, invasion, apoptotic resistance and induction of angiogenesis in cancers *via* transcriptional upregulation of multiple NF-κB downstream genes, such as matrix metalloproteinase (MMPs), B-cell lymphoma (BCLs) and vascular endothelial growth factor (VEGF) [5–8]. A better understanding of the molecular mechanisms underlying the deregulated activation of the NF-κB signaling pathway in cancer would benefit the identification of novel diagnostic and therapeutic targets.

NF-κB transcription factor family comprises NFKB1 (p50/p105), NFKB2 (p52/p100), RelA (p65), c-Rel, and RelB, which form various homo- and heterodimers [9,10]. The NF-κB family of proteins shares an amino terminal 300 amino acid domain, Rel homology domain (RHD), including DNA-binding (DB) and dimerization domains (DD), and the nuclear translocation sequence (NLS), which is the binding site of NF-κB inhibitor (IκBs) for the negative feedback loop [11,12]. NF-κB is sequestered in a quiescent form in the cytoplasm by interacting with its inhibitory proteins, IκB proteins (IκBα, IκBβ and IκBε) or the precursor proteins p100 and p105 [13]. IκBα functions in part by masking a conserved NLS that is found in the RHD of NF-κB, which also contains a nuclear export sequence (NES) that causes the rapid export of such complexes back to the cytoplasm [14]. Importantly, IκBα is also the one of major downstream targets of NF-κB signaling pathway, which plays an important role in termination of NF-κB activation *via* the negative feedback mechanism [15–18]. However, the underlying mechanism by which the NF-κB/IκBα negative feedback loop was disrupted in cancer, resulting in NF-κB pathway constitutively activated, remains largely unclear.

PIMREG, located at 17p13.2, was first identified as a clathrin assembly lymphoid myeloid leukemia gene (CALM) interactor that influences the subcellular localization of the leukemogenic fusion protein CALM/AF10 [19]. Furthermore, PIMREG was found to be highly expressed in leukemia, lymphoma and tumor cell lines but not in non-proliferating T-cells or human peripheral blood lymphocytes [19,20]. Importantly, the results in these studies showed that PIMREG could be induced by mitogens and its protein level is cell cycle-dependent, suggesting a crucial role of PIMREG in regulation of cell proliferation [20]. Moreover, *Barbutti* and colleagues demonstrated that PIMREG played an essential role in enhancement of tumorigenicity in leukemia cell lines [21]. In addition, it has been found PIMREG may promote the breast cancer progression, especially the basal-like subtype, and knockdown of PIMREG significantly suppressed the proliferation capacity of breast cancer cells [22]. However, the precise molecular mechanism of PIMREG in breast cancer aggressiveness remains largely unknown.

The present study showed that PIMREG overexpression in breast cancer sustained NF-κB activity by inhibiting the NF-κB/IκBα negative feedback loop *via* competitively binding to RHD of NF-κB with IκBα. The overexpression of PIMREG in breast cancer strongly correlated with the clinical characteristics of patients with breast cancer. Ectopic expression of PIMREG dramatically promoted the aggressiveness of breast cancer cell, both *in vitro* and *in vivo*. These results provide new insights into the oncogenetic role of PIMREG in constitutive activation of NF-κB signaling in breast cancer aggressiveness.

2. Material and methods

2.1. Cells and cell culture

Primary normal mammary epithelial cells (NMECs) were established according to a previous report [23]. MCF10A, a non-tumorigenic epithelial cell line, was purchased from the American Type Culture Collection (ATCC, Manassas, VA) and cultured in keratinocyte serum free medium (KSFM) supplemented with 0.1 ng/ml human recombinant epidermal growth factor and 20 μg/ml bovine pituitary extract (Invitrogen, Carlsbad, CA). Breast cancer cell lines were purchased from the ATCC, and cultured in Dulbecco's modified Eagle's medium (DMEM) (Gibco, Grand Island, NY) supplemented with 10% FBS (HyClone, Logan, UT) and 100 units of penicillin-streptomycin at 37 °C with 5% CO_2 atmosphere in a humidified incubator. NF-κB inhibitor JSH23 (HY-13982) was purchased from MedChemExpress and dissolved in DMSO to obtain 10 mM stock concentrations, then added to the cell cultured medium to inhibit NF-κB transcriptional activity.

2.2. Patient information and tissue specimens

This study was conducted on seven pairs of breast cancer tissues and the matched adjacent non-tumor tissues, and 212 paraffin embedded breast cancer samples, which were diagnosed histopathologically and clinically at the Sun Yat-sen University Cancer Center. The breast cancer tissues and the matched adjacent non-tumor tissues were frozen and stored in liquid nitrogen until use. For the clinical materials used, prior consent and approval from the Institutional Research Ethics Committee (IREC) were obtained. Clinical and clinicopathological classification and stage were determined according to the American Joint Committee on Cancer (AJCC) criteria. The clinical information on the patients' samples is shown in Supplementary Table 1–4.

2.3. RNA extraction, reverse transcription, and quantitative real-time PCR (qPCR)

Total RNA was extracted from freshly frozen samples or cells using the TRIzol reagent (Invitrogen) [24] and reverse transcribed using a First Strand cDNA Synthesis Kit (Invitrogen). The qPCR was conducted using Platinum SYBR Green qPCR SuperMix-UDG reagents (Invitrogen) on an ABI Prism 7500 Sequence Detection System (Applied Biosystems, Foster City, CA). *GAPDH* was used as the endogenous control and the $2^{-\Delta\Delta CT}$ method was used to calculate the relative expression levels. All reactions were performed in triplicate and the primers used are shown in Supplementary Table 5.

2.4. Western blotting (WB) analysis

Equal quantities of cellular proteins, prepared in sample lysis buffer [25] and heated for 10 min at 100 °C, were electrophoresed through a 10% SDS/polyacrylamide gel and transferred to polyvinylidene fluoride membranes (Millipore, Billerica, MA). The membranes were incubated with anti- PIMREG (also named FAM64A) (1:1000, Cat# ab118102), anti-IKKα (Cat#ab32041), anti- phospho-IKKα (Cat# ab38515), anti-IKKβ (Cat#ab 32135), and anti- phospho-IKKβ (Cat# ab194519) (1:1000, Abcam, Cambridge, MA); and anti-NF-κB/p65 (Cat# 8242), anti- Histone H3 (Cat# 4499), anti-IκBα (Cat# 7543), anti- phospho-IκBα (Cat# 2859), anti-β-actin (Cat# 4970) and anti-α-Tubulin (Cat# 2125), anti- GAPDH (Cat# 5174) antibodies (1:1000; Cell Signaling Technology, Danvers, MA).

2.5. Immunohistochemical (IHC) assay

Formalin-fixed paraffin-embedded tissues were analyzed using immunohistochemical staining as previously described [26,27], using anti-PIMREG antibodies (1:500, Cat# HPA049934, Sigma, St. Louis, MO). Two independent pathologists, blinded to the histopathological features and patient data, separately reviewed and scored the degree of immunostaining of the sections. The proportion of tumor cells was scored as follows: 0 (no positive tumor cells), 1 (<10% positive tumor cells), 2 (10–50% positive tumor cells), and 3 (> 50% positive tumor cells). The intensity of staining was graded according to the following criteria: 0 (no staining), 1 (weak staining = light yellow), 2 (moderate staining = yellow brown), and 3 (strong staining = brown). The staining index (SI) was calculated as the staining intensity score proportion of positive tumor cells. The expression of PIMREG was evaluated by determining the SI, with scores as 0, 1, 2, 3, 4, 6, and 9. The median value (SI = 4) was chosen as the cut off value; samples with SI ≥ 4 were determined as high expression and samples with SI < 4 were determined as low expression. The images were captured using the AxioVision Rel.4.6 computerized image analysis system (Carl Zeiss Co. Ltd., Jena, Germany).

2.6. Vectors, retroviral infection, and transfection

pMSCV- PIMREG was generated by subcloning the PCR-amplified human *PIMREG* coding sequence into vector pMSCV (Clontech, Mountain View, CA). Breast cancer cells were transduced with lentivirus particles expressing PIMREG or a short hairpin RNA (shRNA) targeting the *PIMREG* sequence (Santa Cruz Biotechnologies, CA), according to manufacturer's instructions. Plasmids were transfected using Lipofectamine 3000 (Invitrogen). Retroviral production and infection were performed as described previously [28]. Stable cell lines expressing PIMREG or PIMREG shRNA were selected for 10 days using 0.5 μg/ml puromycin 48 h after infection. HA-tagged full-length p65 and the truncated p65 fragments plasmids were constructed by ViGene BioScieneces company (Shandong, China).

2.7. Xenografted tumor model, H&E, and IHC staining

BALB/c-nude mice (female, 4–5 weeks of age, 18–20 g) were purchased from the Center of Experimental Animal of Guangzhou University of Chinese Medicine. All experimental procedures were approved by the Institutional Animal Care and Use Committee of Guangzhou Medical University. The BALB/c nude mice were randomly divided into two groups for orthotopic implants. One group was inoculated subcutaneously with MDA-MB-231-Vector cells (3×10^6) in the left mammary fat pad and with MDA-MB-231- PIMREG cells (3×10^6) in the right mammary fat pad. The other group was inoculated subcutaneously with MDA-MB-231-RNAi-Vector cells (3×10^6) in the left mammary fat pad and with MDA-MB-231- PIMREG -RNAi cells (3×10^6) in the right mammary fat pad. Images were captured using an *in vivo* bioluminescence imaging system (Xenogen IVIS Spectrum). Tumor volume was calculated using the equation (Length (L) × width $(W)^2$)/2. Thirty days after tumor implantation, the mice were killed, and the mammary tumors were removed and weighed.

Another four groups of mice were inoculated subcutaneously with MDA-MB-231 cells transduced by Vector, PIMREG, RNAi-Vector, or PIMREG -RNAi cells (3×10^6), respectively. Images of lung metastasis were captured at time points when the tumors of each group reached a similar size to control for the effect of tumor growth. Finally, the lungs were collected to count surface metastases under a dissecting microscope. Lungs were fixed in formalin and embedded in paraffin using the routine method. Serial 6.0-μm sections were cut and subjected to hematoxylin and eosin (H&E) staining with Mayer's hematoxylin solution, or analyzed using IHC with anti- PIMREG (Sigma Cat# HPA049934), anti-Ki67 (Cell Signaling Technology Cat# 9449), anti-MMP9 (Cell Signaling Technology Cat# 13667), and anti-NF-κB/p65 (Cell Signaling Technology Cat# 8242) antibodies.

2.8. 3-(4, 5-Dimethyl-2-thiazolyl)-2, 5-diphenyl-2H-tetrazolium bromide (MTT) assay

Cells were seeded in 96-well plates at 0.2×10^4/well. At each time point, cells were stained with 100 μl of sterile MTT dye (0.5 mg/ml, Sigma) for 4 h at 37 °C, followed by removal of the culture medium and addition of 150 μl of dimethyl sulfoxide (Sigma). The absorbance was measured at 490 nm with a spectraphotometric plate reader. All experiments were performed in triplicate.

2.9. Colony formation assay

Cells were plated at 500 cells per well in six-well plates and cultured for 14 days. Colonies were fixed with 10% formaldehyde for 15 min, stained with 0.5% crystal violet for another 15 min, and counted under an inverted microscope. All experiments were performed in triplicate.

2.10. Soft agar clonogenic assay

The anchorage-independent growth ability of cells was determined by soft agar clonogenic assay. Cells (1×10^3) were trypsinized and suspended in 2 ml of complete medium plus 0.33% agar (Sigma). The agar-cell mixture was plated on top of a bottom layer comprising complete medium with 0.66% agar. After 10 days, colony sizes were measured using an ocular micrometer. Colonies >0.1 mm in diameter were scored. All experiments were performed in triplicate.

2.11. Wound healing assay

Cell migration ability was measured using the scratch assay. Briefly, cells were seeded on six-well plates with DMEM containing no FBS and grown to monolayer confluence. The monolayers were scratched with a sterile pipette tip to create straight wounds and then incubated with DMEM containing 10% FBS. At 0 and 24 h after wounding, images

were captured and migration was documented using an inverted Olympus IX50 microscope.

2.12. Transwell matrix penetration assay

Cells (1×10^4) were plated on the top side of polycarbonate Transwell filters coated with Matrigel in the upper chamber of BioCoat™ Invasion Chambers (BD Biosciences, Bedford, MA) and incubated at 37 °C for 22 h, followed by removal of cells inside the upper chamber using cotton swabs. Invaded cells on the lower membrane surface were fixed in 1% paraformaldehyde, stained with hematoxylin, and counted (ten random fields per well, 100 × magnification).

2.13. Co-immunoprecipitation and mass spectrometry (co-IP/MS) analysis

For Immunoprecipitation, dynabeads coupled with HA-antibody was prepared and mixed with cell lysates, which harvested from MDA-MB-231 breast cancer cells transfected with HA-tagged p65-F2, and rotated at 4 °C for 1 h. Immuno-complexes separated from dynabeads were washed with lysis buffer and then suspended with SDS blue loading buffer. Lysis was performed under 70 °C for 10 min and WB analysis was used to detect proteins. Mass spectrometry analysis was further performed by Wininovate Bio. Company (Shenzhen, China).

2.14. Luciferase assay

Luciferase assay was performed according to previous reports [23]. In brief, Cells (1×10^4) were seeded in 48-well plates in triplicate and allowed to settle for 24 h. 100 ng of NF-κB luciferase reporter plasmids or the control plasmid, plus 1 ng of pRL-TK Renilla plasmid (Promega, Madison, WI), were transfected into cells using the Lipofectamine 2000 reagent (Invitrogen) according to the manufacturer's instruction. Luciferase and Renilla signals were measured using the Dual Luciferase Reporter Assay Kit (Promega) according to the manufacturer's protocol.

2.15. Chromatin Immunoprecipitation (ChIP) assays

ChIP assays were conducted using a ChIP assay kit (Invitrogen) according to the manufacturer's instructions. Briefly, chromatin from cross-linked cells was sheared by sonication and incubated overnight with specific antibodies (Acetyl-Histone H3, Cell Signaling Technology) followed by incubation with protein G-Sepharose saturated with salmon sperm DNA. Precipitated DNA and input DNA were analyzed using qPCR, and the results were presented as normalization to the input DNA. The primers for the human interleukin (IL)-6 promoter were: 5′- AGACATGCCAAAGTGCTGAGT-3′ and 5′-GGCTAGCGCTAAGA AG CAGA-3′.

2.16. Nuclear protein extraction assay

The nuclear protein extraction assay was performed using a Nuclear Extraction Kit (Thermo Fisher Scientific, MA). Briefly, cells (5×10^6) were collected, gently resuspended with 500 μl of 1× Hypotonic Buffer, and incubated on ice for 15 min. Then, 25 μl detergent buffer (10% NP40) was added and the homogenate was vortexed for 10 s. The homogenate was centrifuged for 10–15 min at 3000 rpm, 4 °C. The pellet was the nuclear fraction. The pellet was resuspended in 50 μl of complete Cell Extraction Buffer for 30 min on ice with vortexing at 10 min intervals. The sample was centrifuged for 30 min at 14,000 ×g, 4 °C. The supernatant (nuclear fraction) was transferred to a clean microcentrifuge tube and store at −80 °C until use.

2.17. Electrophoretic mobility shift assay (EMSA)

EMSA was performed using a LightShift Chemiluminescent EMSA kit from Pierce Biotechnology (Rockford, IL) according to the manufacturer's instructions. DNA probes containing specific binding sites were used: NF-κB: sense, 5′-AGTTGAGGGGACTTTCCC AGGC-3′, antisense, 5′-GCCTGGGAAAGTCCCCT CAAC-3′; OCT-1 (used as the negative control): sense, 5′-TGTCGAATGCAAATCACTAGAA-3′, antisense, 5′-TTCTAG TGATTT G CATTCGACA-3′.

2.18. Far-Western blot analysis

The indicated proteins were immunoprecipitated by HA-tag affinity gel (Sigma) and resolved by SDS-PAGE, and the proteins were transferred to a polyvinylidene fluoride membrane. The membrane was then blocked in 10% skimmed milk for 1 h at 4 °C. As indicated, recombinant GST-PIMREG was added at 10 μg/ml and incubated at 4 °C for 22 h. The membrane was then washed 6 times with TBST and subjected to western blotting analysis using anti-GST antibody (Sigma) and anti-HA antibody (Sigma).

2.19. Statistical analysis

Data were analyzed statistically using Fisher's exact test, Chi-square test, and Student's two-tailed *t*-test. Survival curves were plotted using the Kaplan-Meier method and compared by the log-rank test. Univariate and multivariate Cox regression analyses were used to determine the significance of various variables for survival. Statistical analyses were performed using the SPSS 11.0 statistical software package. Data represent mean ± SD and $P \leq .05$ was considered statistically significant.

3. Results

3.1. Identification of PIMREG as an activator of NF-κB pathway

The sustained NF-κB signaling activation in cancer was always due to the inefficiency of the negative feedback of IκBα to NF-κB. The NF-κB/p65 RHD domain fragment (F2: 190-321aa), which is the IκBα-binding region [14,29], was constructed to indentfy the potential NF-κB-interacting protein analyzed by co-immunoprecipitation and mass spectrometry (co-IP/MS) (Fig. 1a–b). As shown in Fig. 1b, PIMREG was identified to be a potent NF-κB/p65 (F2)-interacting protein, which suggested that PIMREG might be involved in the regulation of NF-κB signaling *via* binding with its RHD domain. Furthermore, co- IP assays and far-western blotting analyses using series of p65 fragments and PIMREG further confirmed that PIMREG only interacted with fragment of p65 containing RHD region (F2: 190–321 aa) (Fig. 1c–d). Both *in vivo* and *in vitro* co-IP assays further demonstrated that PIMREG physically interacted with NF-κB/p65 (Fig. 1e–f; Supplementary Fig. S1a). Interestingly, we found that the PIMREG/NF-κB interaction only occurred in nucleus but not in cytoplasm (Fig. 1g), which is consistent with PIMREG nuclear location in the breast cancer cells and tissues (Supplementary Fig. S1b-d).

In consistent with this hypothesis, the gene set enrichment analysis (GSEA) analysis revealed that *PIMREG* mRNA expression positively correlated with NF-κB activation (Supplementary Fig. S1e). Furthermore, we found that PIMREG overexpression significantly enhanced, whereas silencing PIMREG reduced, the transcriptional activity, nuclear accumulation and DNA-binding activity of NF-κB, as well as the mRNA levels of multiple NF-κB downstream targets (Fig. 1h–j and Supplementary Fig. S1f-i). Moreover, ChIP assays revealed that ectopic PIMREG promoted the enrichment of H3K27ac on the promoter of *IL6* (interleukin-6), which is well-known the targeted gene of NF-κB/p65 (Supplementary Fig. S1j). Collectively, these results indicate that PIMREG could be an activator of NF-κB pathway.

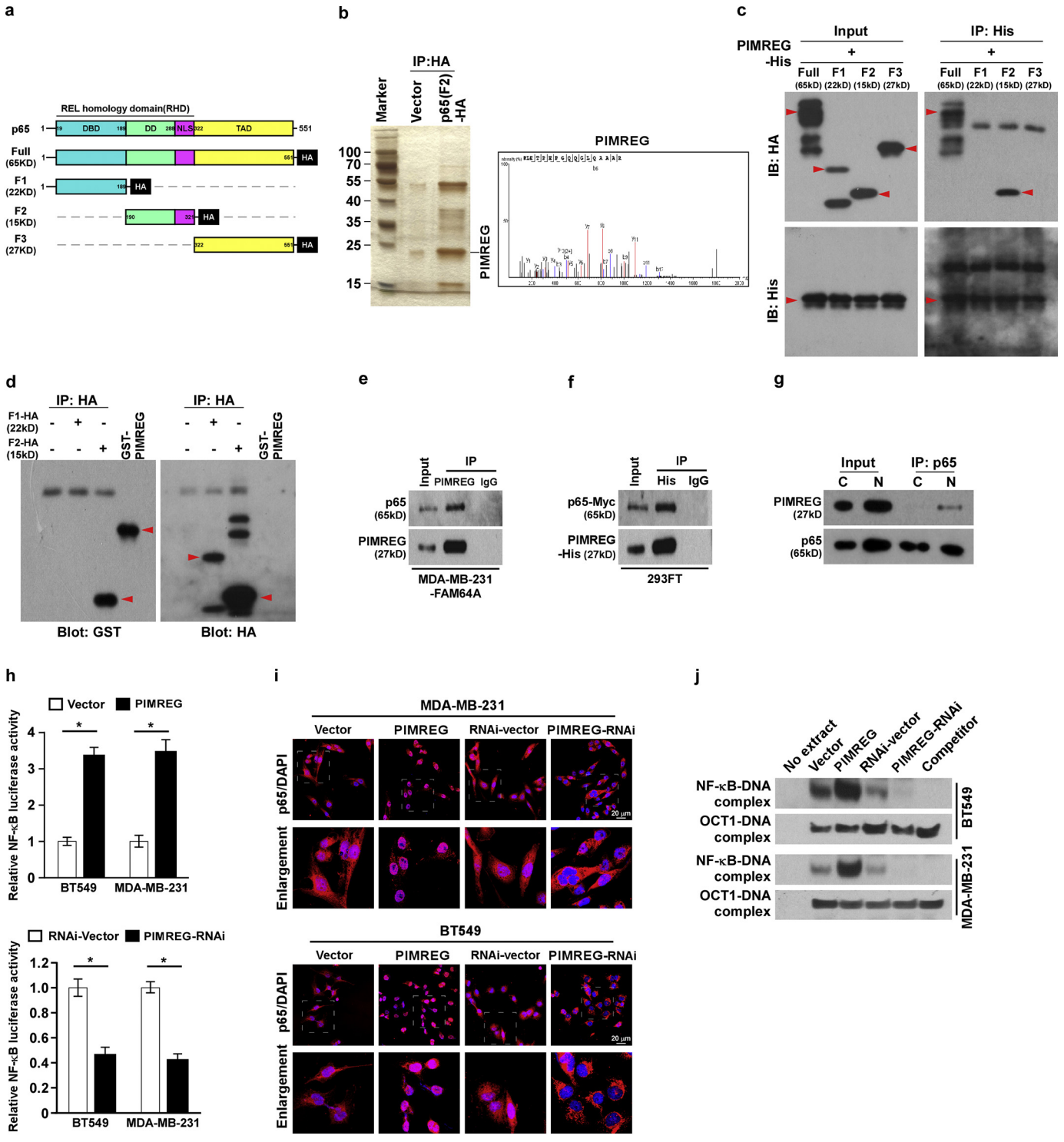

Fig. 1. PIMREG is an activator of NF-κB pathway. (a) Schematic illustration of HA-tagged full-length p65 and three truncated p65 fragments. (b) Lysates from MDA-MB-231 cells transfected with p65 (F2)-HA were immunoprecipitated using anti-HA affinity agarose, followed by MS peptide sequencing. (c) IP analysis showing that PIMREG interacts with F2 fragment of p65; antibodies against HA and His were used to perform co-IP. (d) Immunoprecipitated HA-tagged F1 and F2 were gel purified, transferred to a membrane, incubated with GST-tagged recombinant PIMREG, and then detected using an antibody specific to GST or the HA tag. Recombinant GST-tagged PIMREG was used as a control. (e) IP analysis showing that PIMREG interacts with NF-κB/p65. Antibodies against p65 and PIMREG were used to perform co-IP. (f) 293FT cells transfected with p65-Myc and PIMREG -His plasmids, antibodies against Myc and His were used to perform co-IP. (g) co-IP assay indicated that the PIMREG/NF-κB interaction occurred in nuclear of TNFα-treated cells. (h) NF-κB luciferase reporter activity was analyzed in the indicated TNFα (2 ng/ml)-treated cells. (i) Subcellular localization of NF-κB/p65 in the indicated TNFα (2 ng/ml)-treated cells, as analyzed by immunofluorescence staining (the lower panel is the enlargement of the indicated merged picture). (j) NF-κB activity determined by EMSA analysis in the indicated TNFα (2 ng/ml)-treated cells. Error bars represent the means ± SD of three independent experiments. *$P < .05$. Two-tailed *t*-test was used for the statistical analysis.

3.2. PIMREG sustains NF-κB signaling activity via interacting with RHD of p65

Further we explored the mechanism of PIMREG to activate NF-κB signaling. We found that PIMREG-transduced cells showed similar expression levels of total and the phosphorylated IKKα, IKKβ, and IκBα protein, indicating that PIMREG dysregulation has no impact on IKK activation (Supplementary Fig. S2a). These results suggested an alternative regulatory mechanism of PIMREG on the NF-κB signaling activity. As expected, overexpression of PIMREG significantly reduced, while silencing PIMREG enhanced, the binding affinity of IκBα to NF-κB (Fig. 2a–c; Supplementary Fig. S2b-c). In contrast, ectopically expressing IκBα repressed the PIMREG-induced NF-κB activity in a dose-dependent manner (Fig. 2d). Taken together, these results suggest that PIMREG may compete with IκBα for NF-κB p65 interaction to sustain the activation of NF-κB in breast cancer cells.

3.3. PIMREG sustains nuclear accumulation and transcriptional activity of NF-κB

Prominently, the time course results of immunofluorescence staining and western blotting both revealed that the TNFα-stimulated-nuclear signals of NF-κB/p65 were dramatically prolonged, even after TNFα-treatment withdrawn, in PIMREG -transduced cells, but quickly decreased in PIMREG-silenced cells (Fig. 3a, Supplementary Fig. S3a-b). Coincidentally, the DNA-binding activity of NF-κB after TNFα treatment was also showed to be dramatically sustained in PIMREG-transduced cells, but markedly declined in PIMREG -silenced cells, compared with that in the control cells (Fig. 3b). These results suggested that PIMREG overexpression sustained NF-κB activation. Consistently, overexpressing PIMREG significantly prolonged the TNFα-induced mRNA expressions of *IL1B*, *IL6*, *CCND1*, and *MMP9*, which fast declined in PIMREG-silenced cells (Supplementary Fig. S3c). All these results further support the hypothesis that PIMREG played an important role in sustaining NF-κB signaling in breast cancer cells.

3.4. Elevated PIMREG correlates with breast cancer progression and prognosis

To determine the biological role of PIMREG in breast cancer, we analyzed the expression of PIMREG in two available published profiles obtained from The Cancer Genome Atlas breast cancer dataset (TCGA; https://cancergenome.nih.gov/) and Onocomine database. As shown in Fig. 4a and Supplementary Fig. 4a and b, *PIMREG* was significantly upregulated in breast cancer tissues compared with that in normal tissues ($P < .001$). Consistently, our results also showed that PIMREG expression, at both transcriptional and translational level, was dramatically elevated in seven breast cancer samples compared with that in the matched adjacent non-tumor tissues (Fig. 4b, c), and in all 12 tested breast cancer cell lines compared with that in NMECs and MCF10A (Fig. 4d, e), as determined by qPCR and western blotting analyses. Taken together, these results indicated that PIMREG is upregulated in breast cancer.

To further evaluate whether elevated PIMREG correlated with clinical breast cancer progression, the expression of PIMREG was examined in 212 archived human breast cancer specimens. Consistently, we found that PIMREG was upregulated in breast cancer tissues compared with normal breast tissues (Supplementary Fig. S4c). Among all the cases, 99 (46.7%) had low PIMREG expression, while 113 (53.3%) had high PIMREG expression (Supplementary Table S1). Furthermore, statistical analyses revealed that PIMREG expression significantly correlated with the clinical stage ($P < .001$), tumor-node-metastasis classification (T: $P = .005$; N: $P < .001$; M: $P = .032$), and vital status ($P < .001$) in patients with breast cancer (Fig. 4f, Supplementary Table S2, 3). Moreover, Kaplan-Meier analysis and log-rank test revealed that higher PIMREG levels were associated with shorter survival time, whereas patients with lower PIMREG expression had a longer survival time ($P < .001$; Fig. 4g, h), which was further confirmed by analysis of both TCGA and Kaplan-Meier plotter dataset (Supplementary Fig. S4d-e). Importantly, the relapse-free survival was also associated with PIMREG expression, which patients with higher PIMREG levels had a shorter relapse-free time, while PIMREG-lower patients had a longer relapse-free time, which was consistent with the results of the analysis using the TCGA databases and GSE12276 (Fig. 4i; Supplementary Fig. S4f-g). And the GSE9195 dataset analysis also showed that PIMREG expression was negatively associated with metastasis-free survival (Supplementary Fig. S4 h). Additionally, univariate and multivariate analyses revealed that the PIMREG expression level was an independent prognostic factor in breast cancer (Supplementary Table S4). Taken together, these results suggest a potential correlation between elevated expression of PIMREG and the progression and poor prognosis of human breast cancer.

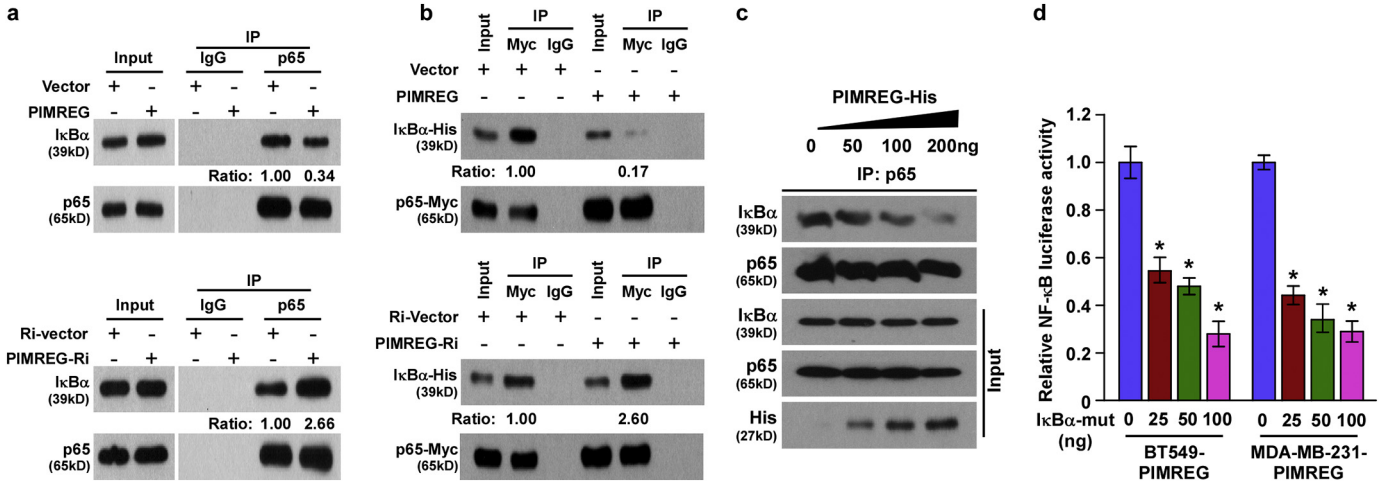

Fig. 2. PIMREG interacts with NF-κB. (a) PIMREG inhibited the binding of NF-κB and IκBα; antibodies p65 and IκBα were used to perform co-IP. (b) Indicated cells transfected with p65-Myc and IκBα-His plasmids, and antibodies against Myc and His, were used to perform co-IP. The optical density value was determined by Quantity One software. Ratio in (a) and (b): the optical density value of IκBα: p65; (c) IP analysis showing that PIMREG interrupted the binding of NF-κB and IκBα in a dose-dependent manner; antibodies against p65 and IκBα were used to perform co-IP. (d) NF-κB luciferase reporter activity was analyzed in PIMREG -transduced cells, treated with IκBα-mut in a dose-dependent manner. Error bars represent the means ± SD of three independent experiments. *$P < .05$. Two-tailed *t*-test was used for the statistical analysis.

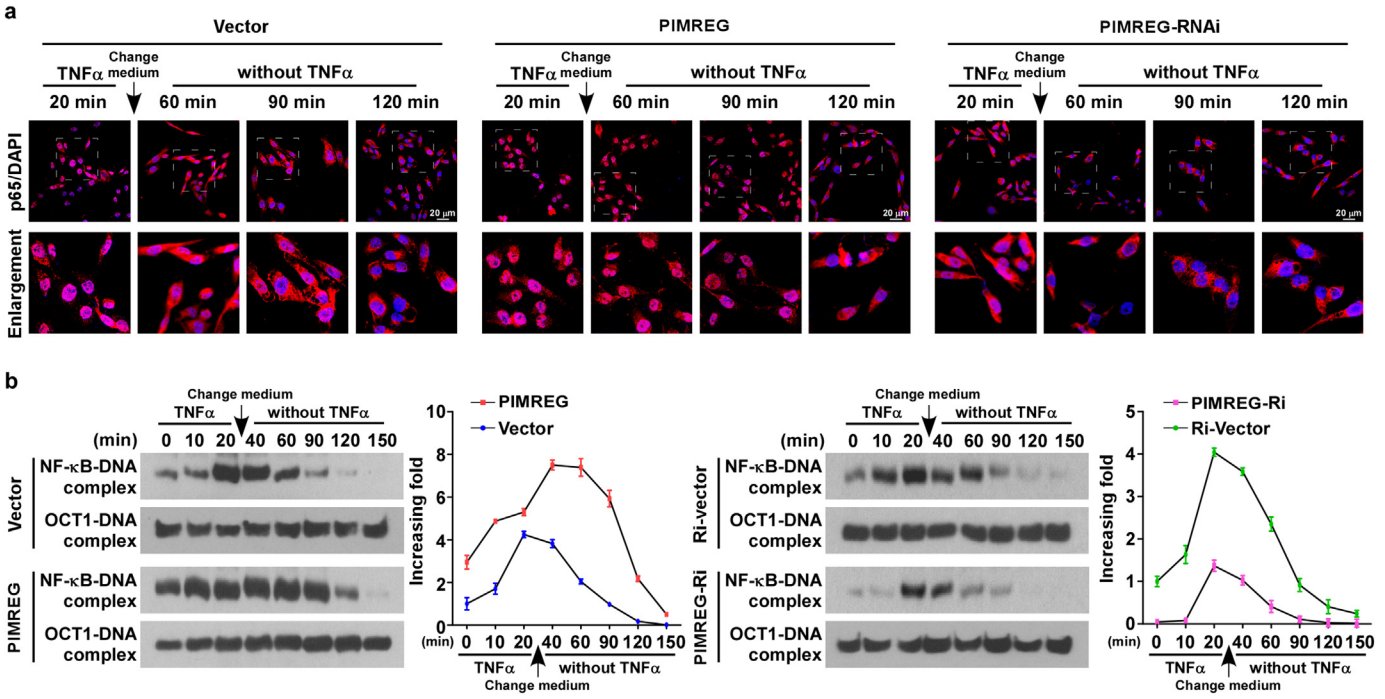

Fig. 3. PIMREG sustains nuclear accumulation and transcriptional activity of NF-κB. (a) Immunofluorescence staining of NF-κB/p65. The lowest panel is the enlargement of the indicated merged picture. (b) NF-κB activity determined by EMSA analysis. The optical density value (right), determined by Quantity One software. Cells were treated with TNFα (10 ng/mL) for 20 min then replaced by medium without TNFα. Error bars represent the means ± SD of three independent experiments. $^{*}P < .05$. Two-tailed *t*-test was used for the statistical analysis.

3.5. PIMREG promotes breast cancer aggressiveness in vivo

Consistent with the results that *PIMREG* expression was significantly upregulated in invasive breast cancer and negatively associated with metastasis-free survival analyzed in the Oncomine database (Supplementary Fig. S4b, h), the GSEA showed that *PIMREG* levels were positively correlated with gene signatures related to invasion and metastasis, as well as cell proliferation and cell cycle, in TCGA breast cancer dataset (Fig. 5a; Supplementary Fig. S5a-c). We then further examined the oncogenic role of PIMREG in breast cancer using an *in vivo* murine model. As shown in Fig. 5b–e, the tumors formed by PIMREG -transduced breast cancer cells were larger, in both size and weight, compared with control tumors, whereas the tumors formed by PIMREG -silenced cells were smaller and lighter than the control tumors. Importantly, the mice bearing PIMREG -transduced tumors displayed prominent lung metastasis, which resulted in shorter survival of mice. Conversely, the capability of MDA-MB-231 cells in lung metastasis was significantly impaired by PIMREG silencing, which the mice implanted with PIMREG -silenced cells survived significantly longer compared with control mice (Fig. 5f–h). Moreover, IHC analysis revealed that PIMREG -transduced tumors exhibited increased percentages of Ki67 (marker of proliferation)-positive cells, MMP9 (represents the invasive ability of breast cancer cells) and nuclear NF-κB expression, whereas PIMREG -silencing tumors displayed lower Ki67, MMP9 and nuclear NF-κB expression (Fig. 5i). Therefore, these data suggest that PIMREG overexpression contributes to breast cancer aggressiveness *in vivo*.

3.6. PIMREG induces breast cancer aggressiveness in vitro

In agreement with the results obtained from *in vivo* experiments, MTT, colony formation and soft agar clonogenic assays revealed that overexpressing PIMREG dramatically increased, but silencing PIMREG decreased, the growth rate of BT549 and MDA-MB-231 cells in both culture dish and soft agar (Fig. 6a–c and Supplementary Fig. S6a-c). Furthermore, we found that the migratory capability of both cells was drastically enhanced by overexpressing PIMREG but suppressed by silencing PIMREG, as determined *via* wound healing assay (Fig. 6d; Supplementary Fig. S6d). Meanwhile, transwell matrix penetration assay revealed that PIMREG-overexpressing cells exhibited substantially increased invasive ability whereas PIMREG-silencing cells displayed reduced invasion capability (Fig. 6e; Supplementary Fig. S6e). Taken together, the results indicate that PIMREG induces breast cancer aggressiveness *in vitro*.

Importantly, blockage of NF-κB signaling using its specific inhibitor JSH23 or IκBα-mut (the IκBα dominant-negative mutant) drastically abrogated the effect of PIMREG overexpression-induced anchorage-independent growth ability and invasive capability of breast cancer cells (Fig. 6f and Supplementary Fig. S6f). These results demonstrated that activation of NF-κB pathway contributed to PIMREG-induced breast cancer aggressiveness.

3.7. Clinical relevance of PIMREG-mediated NF-κB activation in breast cancer

Finally, we examined whether PIMREG-induced NF-κB signaling activation in breast cancer cells was clinically relevant. As shown in Fig. 7a–b, IHC statistical analysis revealed that PIMREG expression was correlated positively with the level of nuclear p65, Ki67, and MMP9 in breast cancer specimens ($P < .05$, respectively). These results were further confirmed in seven freshly collected breast cancer samples compared with one normal breast tissue, in which PIMREG levels were correlated positively with the DNA-binding activity of NF-κB, as determined by EMSA analysis ($r = 0.801$, $P = .017$), and the mRNA expression of NF-κB downstream targets, including *CCND1* ($r = 0.783$, $P = .022$) and *MMP9* ($r = 0.724$, $P = .043$) (Fig. 7c, d). These results further supported the notion that PIMREG overexpression constitutive activates NF-κB signaling, consequently resulting in breast cancer aggressiveness and poorer clinical outcomes (Fig. 7e).

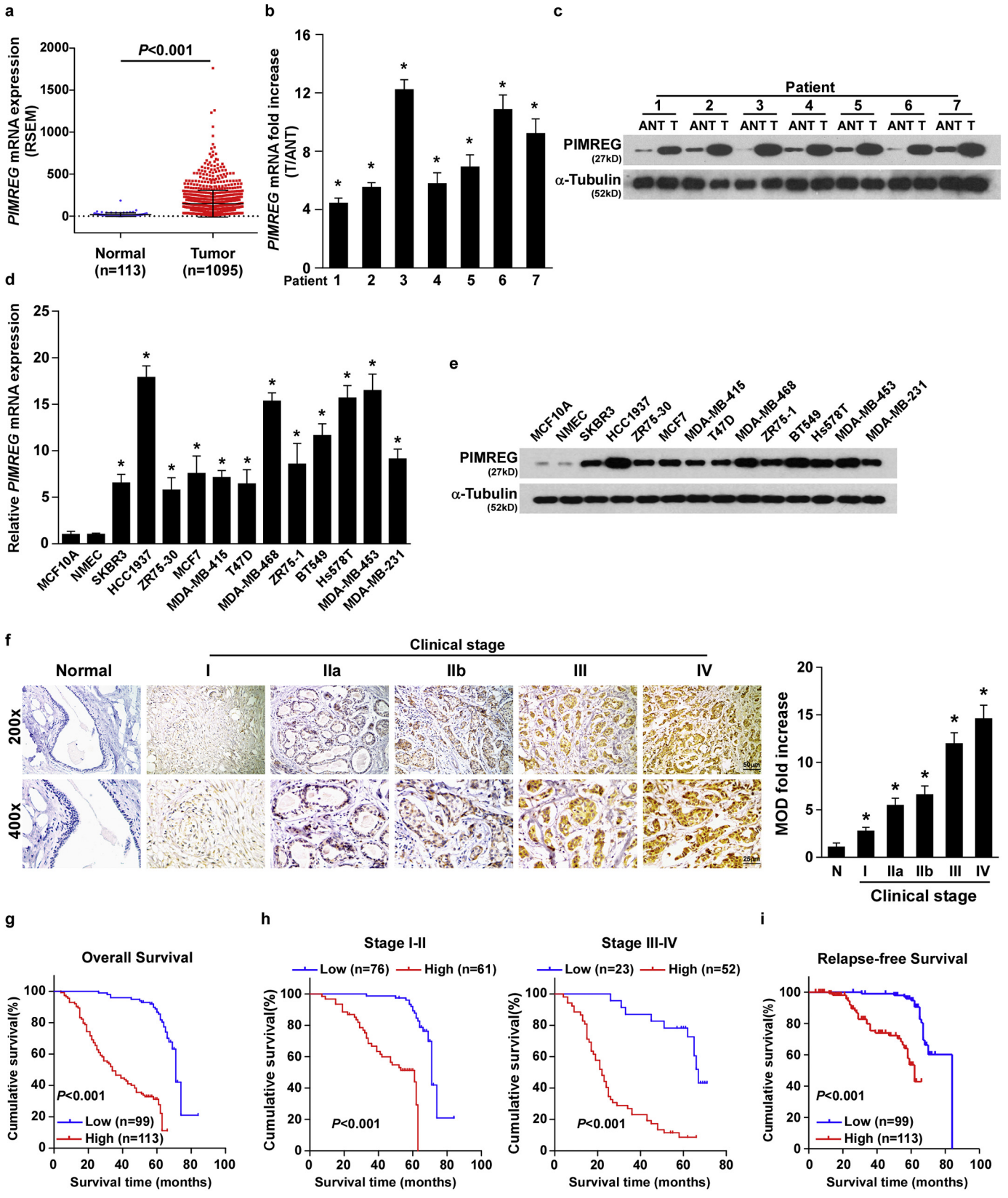

Fig. 4. PIMREG is upregulated in breast cancer and correlates with breast cancer progression and patients' survival. (a) Quantification of *PIMREG* mRNA expression in 1095 breast cancer specimens *vs.* 113 normal breast tissues from TCGA ($P < .001$). RSEM, RNA-seq by Expectation Maximization. (b-c) qPCR (b) and western blotting (c) analysis of PIMREG expression in seven paired breast cancer tissues (T) and the matched adjacent non-tumor tissues (ANT). (d-e) qPCR (d) and western blotting (e) analysis of PIMREG expression in breast cancer cell lines compared with that in MCF10A and NMEC cells. (f) Representative images (left) of IHC analyses of breast cancer specimens (clinical stage I–IV tumors) compared with normal breast tissue (upper, × 200; lower, × 400), and statistical quantification of the average mean optical density (MOD) of PIMREG staining (right). (g) Kaplan–Meier analysis of overall survival for patients with breast cancer stratified by low *vs.* high expression of PIMREG. (h) Kaplan–Meier analysis of overall survival for patients in the clinical stage I and II (left) or clinical stage III and IV (right) subgroups. (i) Kaplan–Meier analysis of relapse-free survival for patients with breast cancer. *P* values were calculated using the log-rank test. Error bar represents the mean ± SD of three independent experiments. * $P < .05$. Two-tailed *t*-test was used for the statistical analysis.

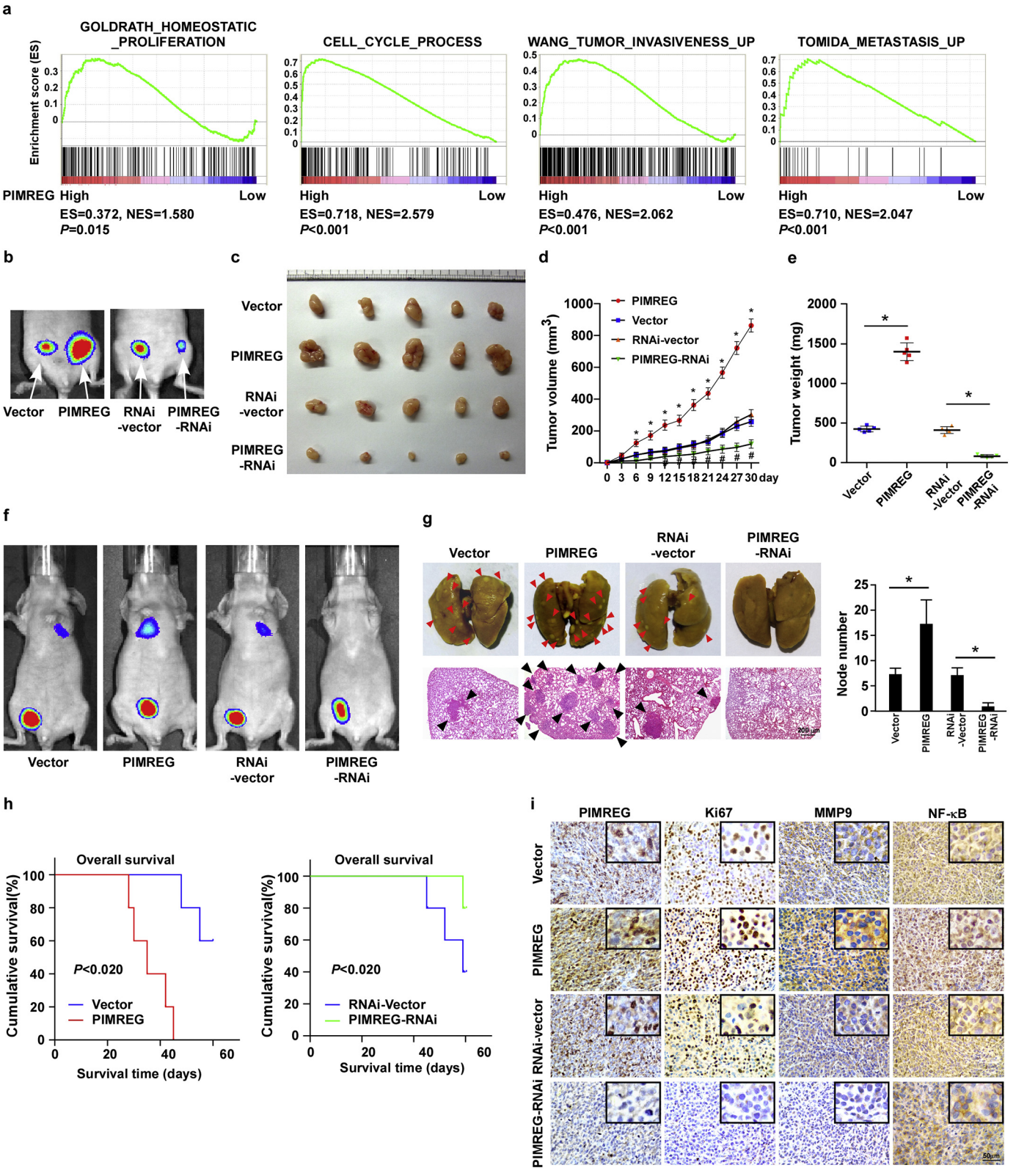

Fig. 5. Elevated PIMREG expression promotes breast cancer cell aggressiveness *in vivo*. (a) The GSEA plots showing that *PIMREG* expression correlated positively with gene signatures related to cell proliferation, cell cycle, invasiveness and metastasis in TCGA breast cancer dataset. ES, enrichment score; NES, normalized enrichment score. (b) Representative *in situ* tumor images of the breast cancer xenograft model in nude mice, captured using the IVIS system. (c) Representative images of the tumors from all the mice in each group. The indicated cells were injected into the mammary fat pad of the mice ($n = 5$/group). (d) Tumor volumes of the indicated groups were measured on the indicated days. (e) Tumor weights of the indicated groups. (f) Representative pictures of *in situ* tumor and lung metastasis, captured using the IVIS system; the time of the images was captured when the tumor of each group reached a similar tumor size. (g) Representative bright field images (left upper), H&E staining (left lower), and quantification (right) of the lung metastases (arrows indicate surface metastatic nodules). (h) Kaplan-Meier curves of the indicated mice groups (log-rank test). (i) IHC staining of PIMREG, Ki67, MMP9, and NF-κB/p65. Each bar represents the mean ± SD of three independent experiments. * $P < .05$. Two-tailed *t*-test was used for the statistical analysis.

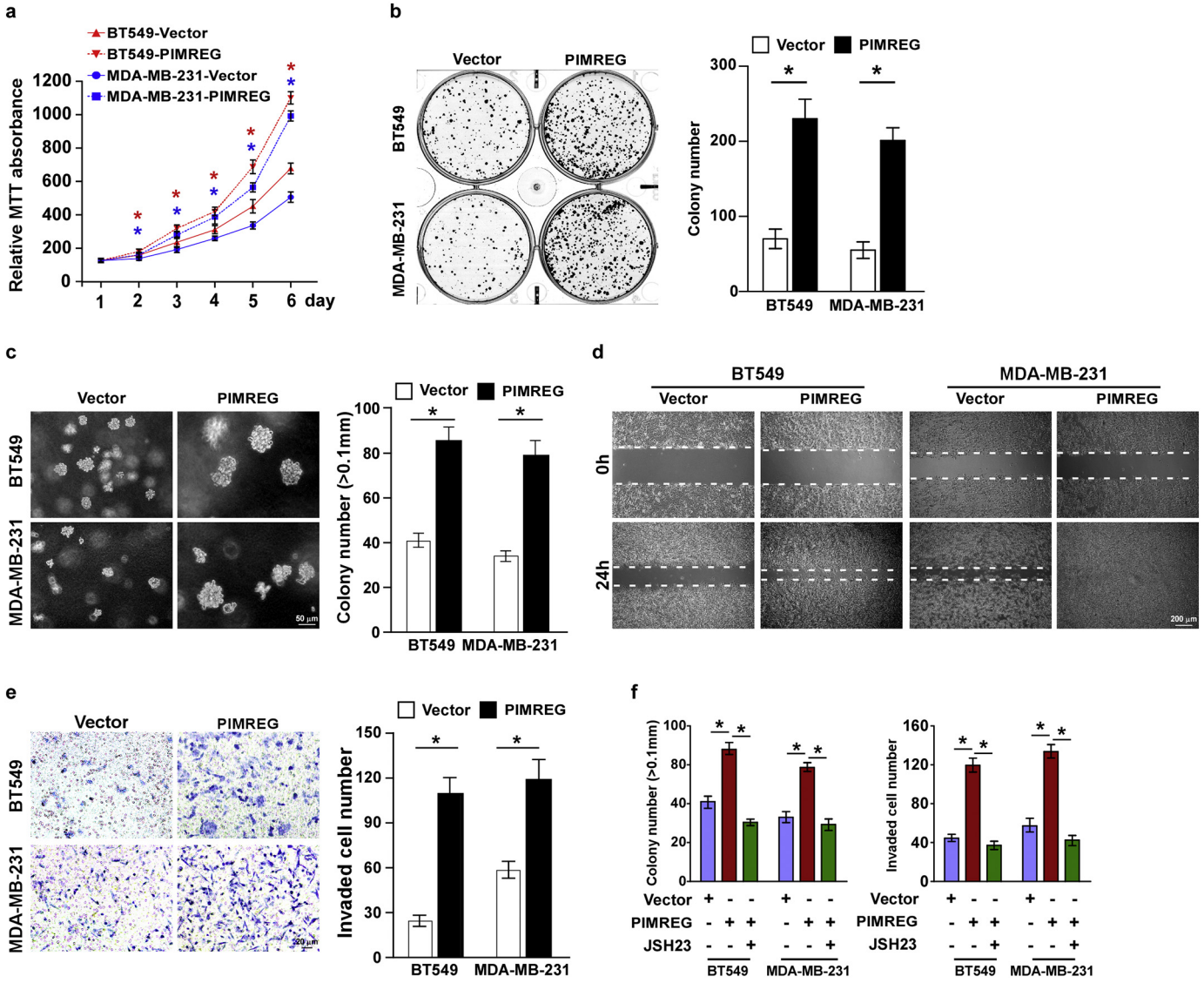

Fig. 6. Elevated PIMREG expression promotes breast cancer cell aggressiveness *in vitro*. (a) MTT analysis of indicated cell growth. (b) Representative images (left) and quantification (right) of colony number of the indicated cells, as determined by a colony formation assay. (c) Representative pictures (left) and quantification (right) of the colony number of the indicated cells, as determined using a soft agar clonogenic assay. Colonies larger than 0.1 mm in diameter were scored. (d) Wound healing assay assessment of the migration of the indicated cells. (e) Representative images (left) and quantification (right) of invaded cells, as analyzed using the transwell matrix penetration assay. (f) Quantification of the colony number determined by soft agar clonogenic assay (left) and invaded cells analyzed using the transwell matrix penetration assay (right), in the indicated cells. Each bar represents the mean ± SD of three independent experiments. * $P < .05$. Two-tailed *t*-test was used for the statistical analysis.

4. Discussion

The key finding of the present study was that PIMREG played crucial roles in promotion of breast cancer aggressiveness *via* constitutive activation of NF-κB signaling pathway. We reported that upregulated PIMREG sustained the NF-κB activation in breast cancer *via* interaction with NF-κB in nucleus and blockage the suppressive function of IκBα on NF-κB. Furthermore, we demonstrated that the expression of PIMREG was markedly upregulated in breast cancer and positively correlated with TNM classification and shorter survival. Therefore, our results provide new insights into the oncogenetic role of PIMREG and uncover novel mechanism in which NF-κB signaling constitutively activates in breast cancer.

Previous studies demonstrated that the IKK complex integrates NF-κB stimuli signals to accelerate the phosphorylation and ubiquitinated degradation of IκBα, followed by nuclear translocation of NF-κB indicating its signaling activation [13,30–32]. On the other hand, IκBα is as well one of the transcriptional targets of NF-κB [15,16]. Newly synthesized IκBα translocates into the nucleus and terminates activated NF-κB-dependent transcription by removing active NF-κB dimers from the DNA and exporting NF-κB back to the cytoplasm to restore the pool of inactive NF-κB/IκBα complex [17,18]. Thus, this negative feedback mechanism controls the physiological activity of NF-κB and prevents the constitutive activation of NF-κB. However, the underlying mechanism by which the NF-κB pathway is constitutively activated in cancer remains largely unclear. In the current study, we demonstrated that PIMREG directly interacted with NF-κB at the RHD (190–321 aa), which contains an NLS that is conditionally masked by IκBα, suggesting that PIMREG may contributed to sustain NF-κB activation *via* blocking the inhibitory function of IκBα to NF-κB. According to the prediction data of *cNLS Mapper* [33] and *NetNES 1.1 Server* [34], there are two predicted NES sites and one predicted NLS domain in the PIMREG protein sequence, indicating the function of PIMREG in mediating NF-κB translocation and activation. Thus, our results uncovered a plausible mechanism in which PIMREG mediated NF-κB activation in cancers.

Previously, Archangelo and colleagues reported that PIMREG interacted with and antagonized the transactivation capacity of CALM/AF10, indicating that PIMREG might functions as transcriptional

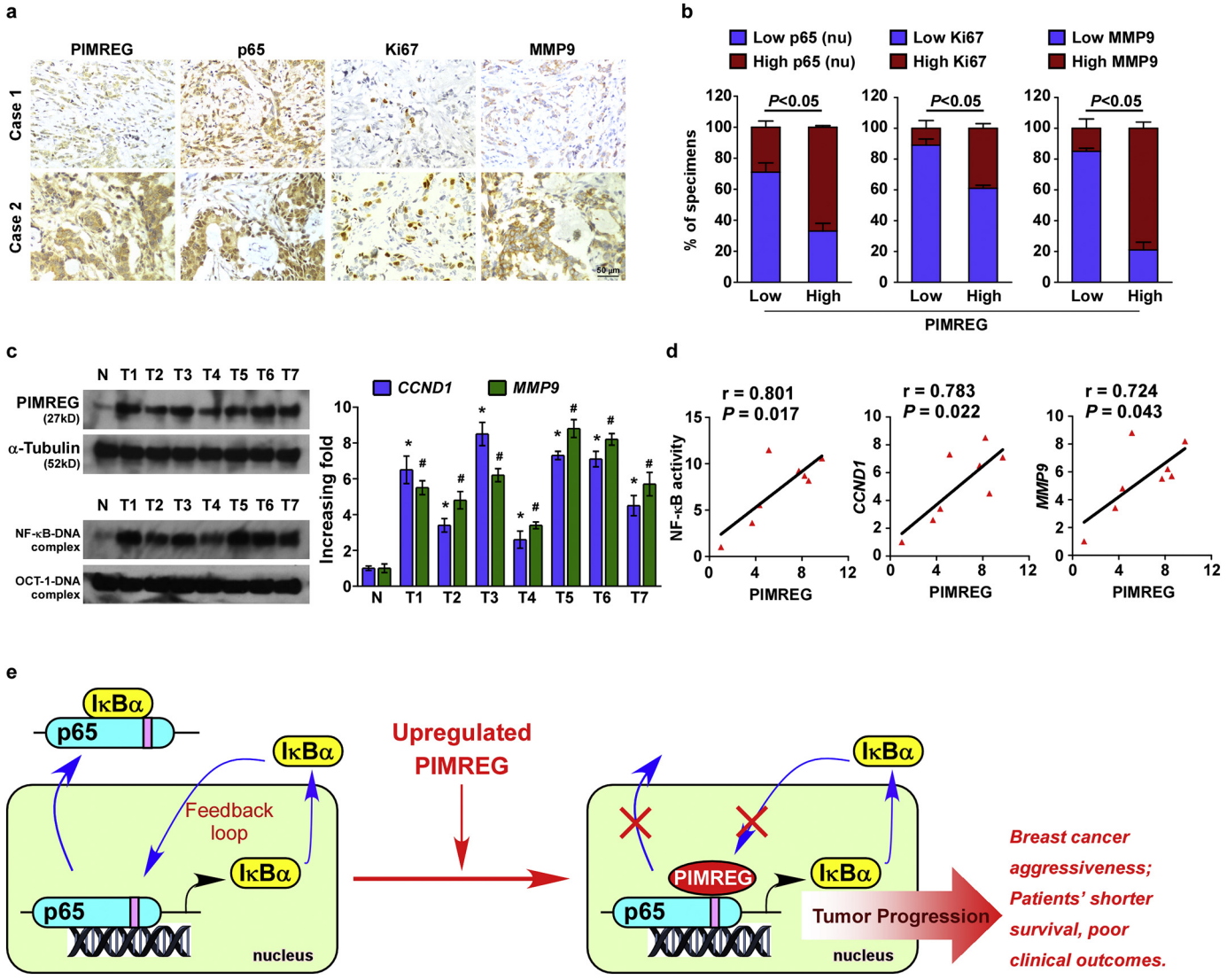

Fig. 7. PIMREG expression correlates clinically with the activation of NF-κB signaling in breast cancer. (a) The expression levels nuclear p65, Ki67, or MMP9, were associated with the expression of PIMREG in primary human breast cancer specimens. Two representative cases are shown, magnification, ×200. (b) Percentage of samples showing low or high nuclear p65, Ki76, or MMP9 expression in primary human breast cancer specimens, relative to the levels of PIMREG. Quantification of IHC was determined using the SI value. (c–d) Western blotting detection of PIMREG expression, EMSA analysis of NF-κB DNA binding activity, and qPCR analysis of *CCND1* and *MMP9* (c), and the correlation analyses of PIMREG expression with the NF-κB DNA binding activity, and *CCND1* and *MMP9* transcriptional expression (d), in seven freshly collected human breast cancer samples, compared with one normal breast tissue. Error bar represents the mean ± SD of three independent experiments. *, # $P < .05$. Two-tailed *t*-test was used for the statistical analysis. (e) The model showing that PIMREG sustained NF-κB activation *via* disrupting the NF-κB/IκBα negative feedback loop, consequently resulting in breast cancer aggressiveness.

repressor [19,35]. Furthermore, Zhao et al. demonstrated that PIMREG could interact with nucleosome remodeling and deacetylase (NuRD) complex [36]. This result might explain the mechanism in which PIMREG acts as transcriptional repressor. However, whether the PIMREG-NuRD complex contributes to antagonize the transactivation capacity of CALM/AF10 need to be further examined since PIMREG could specifically interacts with NuRD complex during mitosis. Meanwhile, Zhao et al. found that PIMREG plays role in control of the timing of the anaphase onset, but they did not observe an obvious change in the levels of global histone deacetylation in PIMREG-depleted mitotic cells *vs.* control mitotic cells, and obvious alteration of spindle checkpoint proteins and G2/M regulators [36], suggesting that the PIMREG-NuRD complex may be involved in remolding of chromatin structure instead of regulation of gene expression. In the current study, we demonstrated that PIMREG competitively interacted with the REL homology domain (RHD) of NF-κB with IκBα, resulted in nuclear accumulation and enhancement of the transcriptional activity of NF-κB. Therefore, PIMREG act as either transcriptional repressor or transcriptional activator might be dependent of different cell cycle and/or interacting-protein, which is worthy to be further investigated.

It has been reported that PIMREG were upregulated in multiple human cancer types [19,20]. We found that PIMREG was also upregulated in breast cancer and upregulated PIMREG was associated with tumor progression and poor patient survival, suggesting that PIMREG might function as an onco-protein in breast cancer and represent a novel and promising prognostic indicator of breast cancer. As the analysis of the TCGA database suggests that the mRNA level of *PIMREG* is upregulated in breast cancer tissues. Zhang et al. reported PIMREG is specifically upregulated in triple-negative breast cancer (TNBC), and higher expression of PIMREG is associated with poorer breast cancer prognosis [37]. Consistently, we also found a relative higher PIMREG expression in series of TNBC cell lines. However, such difference was not achieved in the data of clinical study cohort. Furthermore, we found an acetylation area at the *PIMREG* promoter region (*http://genome.ucsc.edu*), suggesting a possible mechanism of PIMREG protein upregulation, which is under investigating currently in our laboratory.

Breast cancer is the most common cause of cancer death in women in China, especially in women younger than 45 years old and accounted for 15% of all new cancers in women [38,39]. Herein, we demonstrated that PIMREG upregulation promoted breast cancer aggressiveness both *in vivo* and *in vitro* by sustaining nuclear accumulation and transcriptional activity of NF-κB *via* interacting with its RHD (190–321 aa), resulting in disrupting the NF-κB/IκBα negative feedback loop. Meanwhile, PIMREG was highly expressed in breast cancer and strongly correlated with patients' progression and poor outcome. Therefore, our results provide new insights into PIMREG's regulatory function on NF-κB activity and breast cancer progression, which suggested that PIMREG might be a potential prognostic factor and therapeutic target in breast cancer.

Acknowledgements

This work was supported by the Natural Science Foundation of China (No. 81830082, 91740119, 81672874, 81621004, 81502194), the Guangdong Province Universities and Colleges Pearl River Scholar Funded Scheme (GDUPS), the Distinguished Young Scholar of Guangdong Province (No. 2015A030306033), the Natural Science Foundation of Guangdong Province (No. 2015A030313468), the Young Scholar of Science and Technology of Guangdong Province (2016TQ03R801), the Innovative Academic Team of Guangzhou Education System (1201610014), the Science and Technology Program of Guangzhou (201604020001, 201803010098), the Natural Science Foundation Research Team of Guangdong Province (2018B030312001), the Research Team of Department of Education of Guangdong Province (2017KCXTD027),the Guangzhou key medical discipline construction project fun, Guangdong Traditional Chinese Medicine Bureau Project (20161178), and Guangzhou Traditional Chinese Medicine and Traditional Chinese and Western Medicine Science and Technology Project (2016A011020; 20182A011025).

Funding sources

The funding institution had no role in the study design, data collection, data analysis, interpretation or writing of the manuscript.

Declaration of interests

The authors have no professional, personal or financial conflicts of interests relating to this publication.

Author contributions

JL developed the original idea and design the study, abstracted and analyzed data, wrote the manuscript, and is the guarantor. LJ and LR contributed to the development of the protocol and prepared the manuscript. XZ, HC, XC and CL performed the *in vitro* biological experiments and data analysis. LW, NH, JP and ZZ performed the *in vivo* experiments and data analysis. DH and JY contributed to clinical data collection and statistical analysis. YL and HH provided the bioinformatics analysis of the study.

Appendix A. Supplementary data

Supplementary data to this article can be found online at https://doi.org/10.1016/j.ebiom.2019.04.001.

References

[1] Hayden MS, Ghosh S. Shared principles in NF-kappaB signaling. Cell 2008;132(3):344–62.
[2] Baldwin AS. Regulation of cell death and autophagy by IKK and NF-kappaB: critical mechanisms in immune function and cancer. Immunol Rev 2012;246(1):327–45.
[3] Chen TL, Tran M, Lakshmanan A, Goettl VM, Lehman AM, et al. NF-kappaB p50 (nfkb1) contributes to pathogenesis in the emu-TCL1 mouse model of chronic lymphocytic leukemia. Blood 2017;130(3):376–9.
[4] Taniguchi K, Karin M. NF-kappaB, inflammation, immunity and cancer: coming of age. Nat Rev Immunol 2018;18(5):309–24.
[5] Jiang L, Lin C, Song L, Wu J, Chen B, Ying Z, et al. MicroRNA-30e* promotes human glioma cell invasiveness in an orthotopic xenotransplantation model by disrupting the NF-kappaB/IkappaBalpha negative feedback loop. J Clin Invest 2012;122(1):33–47.
[6] Jiang L, Wu J, Yang Y, Liu L, Song L, Li J, et al. Bmi-1 promotes the aggressiveness of glioma via activating the NF-kappaB/MMP-9 signaling pathway. BMC Cancer 2012;12:406.
[7] Jiang L, Song L, Wu J, Yang Y, Zhu X, Hu B, et al. Bmi-1 promotes glioma angiogenesis by activating NF-kappaB signaling. PLoS One 2013;8(1):e55527.
[8] Cai Z, Tchou-Wong KM, Rom WN. NF-kappaB in lung tumorigenesis. Cancers 2011;3(4):4258–68.
[9] Rothgiesser KM, Fey M, Hottiger MO. Acetylation of p65 at lysine 314 is important for late NF-kappaB-dependent gene expression. BMC Genomics 2010;11:22.
[10] Hayden MS, Ghosh S. NF-kappaB, the first quarter-century: remarkable progress and outstanding questions. Genes Dev 2012;26(3):203–34.
[11] Baeuerle PA. IkappaB-NF-kappaB structures: at the interface of inflammation control. Cell 1998;95(6):729–31.
[12] Verma IM, Stevenson JK, Schwarz EM, Van Antwerp D, Miyamoto S. Rel/NF-kappa B/I kappa B family: intimate tales of association and dissociation. Genes Dev 1995;9(22):2723–35.
[13] Hinz M, Scheidereit C. The IkappaB kinase complex in NF-kappaB regulation and beyond. EMBO Rep 2014;15(1):46–61.
[14] Perkins ND. Integrating cell-signalling pathways with NF-kappaB and IKK function. Nat Rev Mol Cell Biol 2007;8(1):49–62.
[15] Chiao PJ, Miyamoto S, Verma IM. Autoregulation of I kappa B alpha activity. Proc Natl Acad Sci U S A 1994;91(1):28–32.
[16] Le Bail O, Schmidt-Ullrich R, Israel A. Promoter analysis of the gene encoding the I kappa B-alpha/MAD3 inhibitor of NF-kappa B: positive regulation by members of the rel/NF-kappa B family. EMBO J 1993;12(13):5043–9.
[17] Arenzana-Seisdedos F, Thompson J, Rodriguez MS, Bachelerie F, Thomas D, Hay RT. Inducible nuclear expression of newly synthesized I kappa B alpha negatively regulates DNA-binding and transcriptional activities of NF-kappa B. Mol Cell Biol 1995;15(5):2689–96.
[18] Turpin P, Hay RT, Dargemont C. Characterization of IkappaBalpha nuclear import pathway. J Biol Chem 1999;274(10):6804–12.
[19] Archangelo LF, Glasner J, Krause A, Bohlander SK. The novel CALM interactor CATS influences the subcellular localization of the leukemogenic fusion protein CALM/AF10. Oncogene 2006;25(29):4099–109.
[20] Archangelo LF, Greif PA, Holzel M, Harasim T, Kremmer E, Przemeck GK, et al. The CALM and CALM/AF10 interactor CATS is a marker for proliferation. Mol Oncol 2008;2(4):356–67.
[21] Barbutti I, Xavier-Ferrucio JM, Machado-Neto JA, Ricon L, Traina F, Bohlander SK, et al. CATS (FAM64A) abnormal expression reduces clonogenicity of hematopoietic cells. Oncotarget 2016;7(42):68385–96.
[22] Hu S, Yuan H, Li Z, Zhang J, Wu J, Chen Y, et al. Transcriptional response profiles of paired tumor-normal samples offer novel perspectives in pan-cancer analysis. Oncotarget 2017;8(25):41334–47.
[23] Jiang L, Yu L, Zhang X, Lei F, Wang L, Liu X, et al. miR-892b silencing activates NF-kappaB and promotes aggressiveness in breast Cancer. Cancer Res 2016;76(5):1101–11.
[24] Jiang L, Zang D, Yi S, Li X, Yang C, Dong X, et al. A microRNA-mediated decrease in eukaryotic initiation factor 2alpha promotes cell survival during PS-341 treatment. Sci Rep 2016;6:21565.
[25] Zhao C, Chen X, Zang D, Lan X, Liao S, Yang C, et al. A novel nickel complex works as a proteasomal deubiquitinase inhibitor for cancer therapy. Oncogene 2016;35(45):5916–27.
[26] Jiang L, Zhou J, Zhong D, Zhou Y, Zhang W, Wu W, et al. Overexpression of SMC4 activates TGFbeta/Smad signaling and promotes aggressive phenotype in glioma cells. Oncogenesis 2017;6(3):e301.
[27] Song J, Xie C, Jiang L, Wu G, Zhu J, Zhang S, et al. Transcription factor AP-4 promotes tumorigenic capability and activates the Wnt/beta-catenin pathway in hepatocellular carcinoma. Theranostics 2018;8(13):3571–83.
[28] Zeng Z, Lin H, Zhao X, Liu G, Wang X, Xu R, et al. Overexpression of GOLPH3 promotes proliferation and tumorigenicity in breast cancer via suppression of the FOXO1 transcription factor. Clin Cancer Res 2012;18(15):4059–69.
[29] Malek S, Huxford T, Ghosh G. Ikappa Balpha functions through direct contacts with the nuclear localization signals and the DNA binding sequences of NF-kappaB. J Biol Chem 1998;273(39):25427–35.
[30] DiDonato JA, Hayakawa M, Rothwarf DM, Zandi E, Karin M. A cytokine-responsive IkappaB kinase that activates the transcription factor NF-kappaB. Nature 1997;388(6642):548–54.
[31] Zandi E, Rothwarf DM, Delhase M, Hayakawa M, Karin M. The IkappaB kinase complex (IKK) contains two kinase subunits, IKKalpha and IKKbeta, necessary for IkappaB phosphorylation and NF-kappaB activation. Cell 1997;91(2):243–52.
[32] Hinz M, Arslan SC, Scheidereit C. It takes two to tango: IkappaBs, the multifunctional partners of NF-kappaB. Immunol Rev 2012;246(1):59–76.
[33] Kosugi S, Hasebe M, Tomita M, Yanagawa H. Systematic identification of cell cycle-dependent yeast nucleocytoplasmic shuttling proteins by prediction of composite motifs. Proc Natl Acad Sci U S A 2009;106(25):10171–6.
[34] la Cour T, Kiemer L, Molgaard A, Gupta R, Skriver K, Brunak S. Analysis and prediction of leucine-rich nuclear export signals. Protein engineering, design & selection. PEDS 2004;17(6):527–36.

[35] Archangelo LF, Greif PA, Maucuer A, Manceau V, Koneru N, Bigarella CL, et al. The CATS (FAM64A) protein is a substrate of the kinase interacting Stathmin (KIS). Biochim Biophys Acta 2013;1833(5):1269–79.
[36] Zhao WM, Coppinger JA, Seki A, Cheng XL, Yates III JR, Fang G. RCS1, a substrate of APC/C, controls the metaphase to anaphase transition. Proc Natl Acad Sci U S A 2008;105(36):13415–20.
[37] Zhang C, Han Y, Huang H, Min L, Qu L, Shou C. Integrated analysis of expression profiling data identifies three genes in correlation with poor prognosis of triple-negative breast cancer. Int J Oncol 2014;44(6):2025–33.
[38] Chen W, Zheng R, Baade PD, Zhang S, Zeng H, Bray F, et al. Cancer statistics in China, 2015. CA Cancer J Clin 2016;66(2):115–32.
[39] Xia C, Kahn C, Wang J, Liao Y, Chen W, Yu XQ. Temporal trends in geographical variation in breast Cancer mortality in China, 1973-2005: an analysis of Nationwide surveys on cause of death. Int J Environ Res Public Health 2016;13(10).